International Journal of Chemical, Materials and Biomolecular Sciences
ISSN: 2415-6620
Vol:10, No:6, 2016

Study of Debonding of Composite Material from a Deforming Concrete Beam Using Infrared Thermography

Igor Shardakov, Anton Bykov, Alexey Shestakov, Irina Glot

***Abstract*—**This article focuses on the cycle of experimental studies of the formation of cracks and debondings in the concrete reinforced with carbon fiber. This research was carried out in Perm National Research Polytechnic University. A series of CFRP-strengthened RC beams was tested to investigate the influence of preload and crack repairing factors on CFRP debonding. IRT was applied to detect the early stage of IC debonding during the laboratory bending tests. It was found that for the beams strengthened under load after crack injecting, CFRP debonding strain is 4-65% lower than for the preliminary strengthened beams. The beams strengthened under the load had a relative area of debonding of 2 times higher than preliminary strengthened beams. The CFRP debonding strain is weakly dependent on the strength of the concrete substrate. For beams with a transverse wrapping anchorage in support sections FRP debonding is not a failure mode.

***Keywords*—**FRP, RC beams, strengthening, IC debonding, infrared thermography, quality control, non-destructive testing methods.

I. Introduction

THERE are several possible options known of failure of composite reinforced concrete beams [1]: FRP rupture, crushing of compressive concrete, shear failure, concrete cover separation, plate end interfacial debonding and intermediate crack induced interfacial debonding. When designing structures, reinforced with composite materials, the strains in the composite are limited by the value corresponding to the onset of delamination of the composite from the concrete base. In the Russian (SP 164.1325800.2014, [2]) and American (ACI 440.2R-08, [3]) regulations, this approach is provided for both bent elements without anchorage of the sheet and for elements with anchorage. In addition, the research was carried out, which shows the influence of the degree of preload on the strength and stiffness of reinforced beams [4]-[6]. However, the issue of how the reinforcement under the load effects on the deformation parameters characterizing delamination, is insufficiently studied. The paper presents the test results of three series of reinforced concrete beams, showing characteristics of delamination of the composite in the beams, reinforced with a carbon fiber sheet before load application and during loading after the appearance of the first cracks and their grouting. The method of infrared thermography was used for the study.

A. A. Bykov is with the Perm National Research Polytechnic University, Komsomolsky ave., 29, Perm, 614990, Russia (e-mail: violentharpy@ya.ru).

I. O. Glot, Jr., and A. P. Shestakov are with Institute of Continuous Media Mechanics of the Ural Branch of Russian Academy of Science (ICMM UB RAS), Korolev str., 1, Perm, 614013, Russia (e-mail: glot@icmm.ru, shap@icmm.ru).

I. N. Shardakov is with ICMM UB RAS, Korolev str., 1, Perm, 614013, Russia (corresponding author; phone: +7-342-2378318; e-mail: shardakov@icmm.ru).

II. Program and Methods of Testing

Concrete beams – samples of concrete B20 (Group B1) and concrete B35 (Group B2), were made to perform the tests. The reinforcing scheme of the samples with steel and a carbon fiber sheet is shown in Fig. 1. Each group of beams (B1 and B2) was divided into 3 series with 3-5 samples in each of them. The "a" series – the reference samples; the «b» series – beams reinforced before load application by the carbon sheet SikaWrap-230 6 cm wide with strap anchorage 20 cm wide on the bearings; the «c» series – beams reinforced by the carbon sheet during loading after the appearance of the first cracks and their grouting. Totally 22 sample-beams were made and tested. The tests were performed on a specially designed four-point bending test set-up, (Fig. 2 (a)). The registration of the longitudinal reinforcement strain was carried out by means of strain gauges.

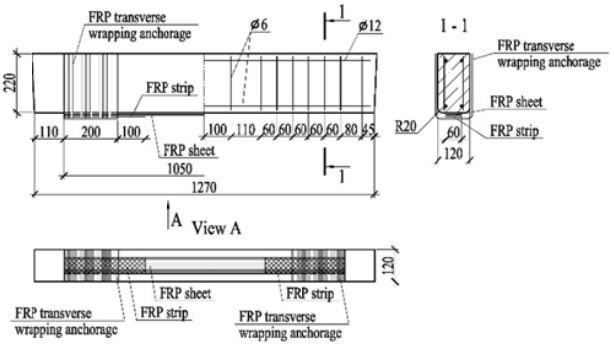

Fig. 1 The reinforcement scheme of beams with steel and carbon fiber sheet

The loading of the beams was performed by a successive increasing quasistatic load with a step of 2 kN, representing 4-6% of the breaking load. At each stage of loading a 5-10-minute stop was performed, during which the pattern of cracks was recorded, as well as their opening width and the heating of the beam was carried out along with the infrared photography of the surface of the carbon fiber sheet [7]-[9] by the infrared imager FLIR T620. The shooting of the stretched

surface of the beam was conducted through the reflection in the mirror, which provided the security of the expensive equipment (Fig. 2 (b)).

The numerical modeling of the heating and cooling processes in the concrete beam strengthened with a carbon strip, made it possible to estimate the change in surface temperature of the entire beam, as well as the beam with delaminations. During the simulation characteristics of the thermal exposure were found, which provide the maximum temperature changes in the beam with debonding (time and power of heating, temperature registration moment). It was found that the maximum temperature response to the presence of delaminations is observed at the cooling of the beam after heating (in the10th second after the start of cooling). [10]

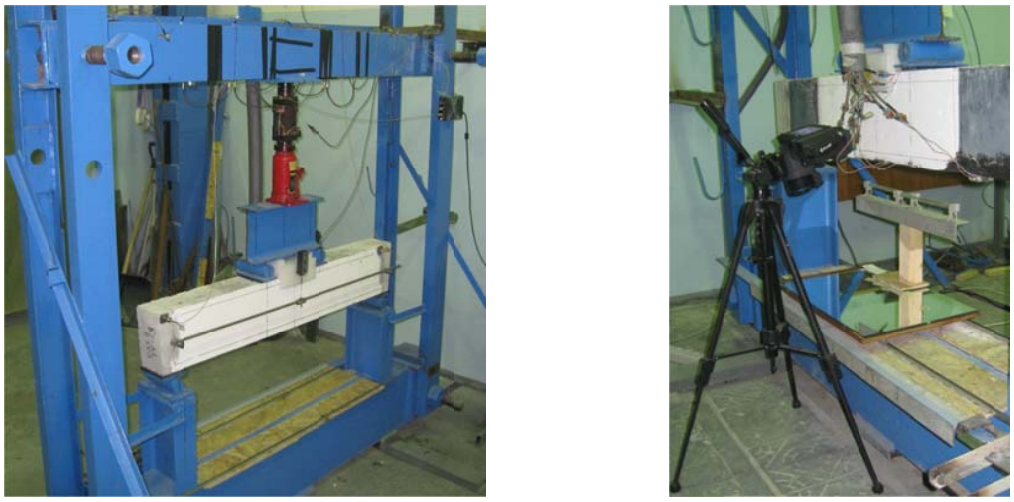

(a) (b)

Fig. 2 Test set-up equipment: the test set-up with a loading tool (a) and the infrared shooting scheme (b)

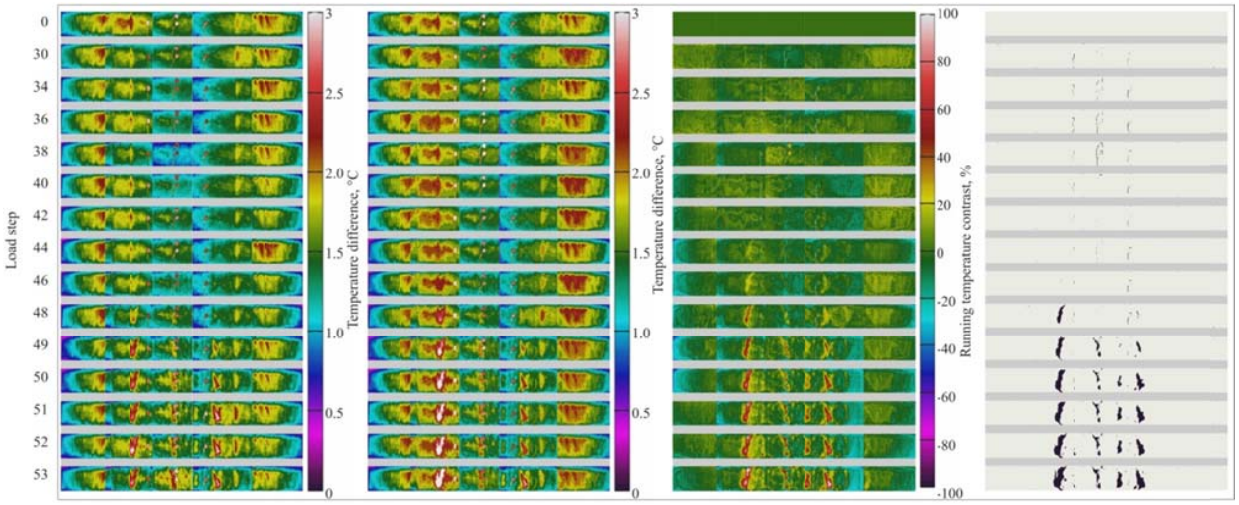

(a) (b) (c) (d)

Fig. 3 Infrared photography transformation algorithm: (a) primary thermogram; (b) normalized thermogram; (c) temperature contrast map; (d) binary card of defects

The primary thermograms of the beam surface (Fig. 3 (a)) were obtained during the tests, which were then transformed by a specially developed algorithm, implemented in the Matlab package. Let us denote as the initial temperature $T(x;y)$ the temperature difference at an arbitrary point (x,y) on the surface of the carbon-fiber layer at the initial time and in the 19th second after the start of observations. The so-called normalized temperature was calculated on the first step of algorithm (Fig. 3 (b)):

$$T_j^n(x,y) = T_j(x,y)\frac{T_0(x_*,y_*)}{T_j(x_*,y_*)} \quad (1)$$

where $T_j(x,y)$ and $T_j^n(x,y)$ – the primary and normalized temperatures at *j*-step of loading at the point (x,y), $T_0(x_*,y_*)$ and $T_j(x_*,y_*)$ – the primary temperatures at the initial step and *j*-step of loading at the point (x_*,y_*) where there is no delamination until the destruction of the beam. Then, the maps of the temperature contrast $C_j(x,y)$ were calculated (Fig. 3 (c)), reflecting the difference of the normalized temperature $T_j^n(x,y)$ at a certain point at the *j*- step of loading and the primary temperature $T_0(x,y)$ at the same point at the initial stage:

$$C_j(x,y)=\frac{T_j^n(x,y)-T_0(x,y)}{T_0(x,y)}\cdot 100\% \quad (2)$$

The increased values of the current temperature contrast indicate the presence of delamination in the given area of the beam. The threshold values of the temperature contrast C^*, separating the defect-free regions from the defect ones, can be obtained by estimating the average contrast value $\overline{C_j}$ and the standard deviation σ_j in those areas of the thermograms, where the presence of defects is excluded. The estimation of these values, obtained according to the data of the tests of all tested beams with a reinforcing layer gives us the following threshold value: $C^*=\overline{C_j}+3\sigma_j=27{,}9\%$. The areas, where the current temperature contrast value does not exceed the threshold value, were identified as defect-free, the rest – as areas with delamination. Fig. 3 (d) presents the obtained in this way binary defect maps, corresponding to successive steps of loading.

III. Results and Discussions

The summary data of the static test results for the beams of the "a" and "b" series are shown in Table I, the "c" series – in Table II, indicating M_{crc} – bending moment corresponding to the first visible cracks appearance, $a_{crc,max}$ – the maximum crack opening width, M_{ult} – the maximum bending moment, f_{ult} – the maximum beam deflection, $\varepsilon_{f,ult}$ – the strain of the carbon-fiber layer at the moment of its break. In a series of preliminary tests actual concrete classes for each beam were determined. For the beams, whose surface had been cleaned with a wire brush before sticking CFRP, the delamination occurred according to the adhesive scenario. For the beams, refined with an abrasive tool to a depth of 2-3 mm, the delamination occurred according to the cohesive scenario. For the non-strengthened beams (the "a" series) the destruction point was determined by the rupture of metal reinforcement and destruction of the concrete in the compressed zone, for the strengthened ones (the "b" and "c" series) – by the rupture of CFRP, in a number of cases accompanied by the rupture of metal reinforcement.

Fig. 4 shows the dependence of the maximum beam deflection on the bending moment obtained for three series of beams: beams without any strengthening layer ("a" series); beams, preliminary strengthened with a carbon-fiber sheet ("b" series) and beams, which underwent the reinforcing procedure while testing ("c" series). The comparison of the graphs obtained in the "a" and "b" series clearly demonstrates an increase in the bearing capacity of the beams strengthened preliminary. The maximum bending moment, which such beams can stand, has happened to be by 37-39% higher than the reference samples. The graphs clearly reflect the appearance of the first cracks in the concrete: it corresponds to a sharp change in the slope angle of the curves.

The designed algorithm of thermogram transformation allows one to estimate the relative area of delamination, accumulated in the beams at a certain step of loading. The data presented in Table III show that the relative area of delamination in the beams reinforced under loading (after healing the first cracks and gluing the sheet) is on average 2.1-2.3 times greater than in the preliminary reinforced ones.

The evolution of deformation in the beams reinforced during loading is of particular interest. At the initial stage of loading such a beam behaves in the same way as a non-strengthened one (Fig. 4, solid thick lines). The appearance of the first cracks in the concrete causes a sharp increase in deformation. The subsequent grouting of cracks in the beam under the load leads to the restoration of its carrying capacity. At this stage, the deformation curve has the "step", on which the slope of the curve is almost restored to its initial value. With a further increase in the bending moment beam displays the same behavior pattern, as the preliminarily reinforced one. The beams strengthened under the load showed an increase in their carrying capacity by 38-49% compared to the non-strengthened samples, and the appearance of the second generation cracks started when the bending moment increased by 45-71%.

In the graphs the loading intervals are marked (circled zones), corresponding to the beginning of cohesive delamination of CFRP. In the beams strengthened under loading delamination begins when the bending moment is on average 75% of the maximum value (Table III). Thus, our tests show that the loss of the bearing capacity of the beam cannot be correlated with the beginning of delamination of the reinforcing layer. As shown in the graphs of Fig. 4, from the beginning of sheet delamination the beam continues to perceive the load and reduction of rigidity does not take place. This means that from the appearance of the first debonding zones to the total loss of the bearing capacity the beam has some strength reserve which is ~ 25% of the ultimate load.

The designed algorithm of thermogram transformation allows one to estimate the relative area of delamination, accumulated in the beams at a certain step of loading. The data presented in Table III show that the relative area of delamination in the beams reinforced under loading (after healing the first cracks and gluing the sheet) is on average 2.1-2.3 times greater than in the preliminary reinforced ones.

TABLE I
THE RESULTS OF STATIC TEST OF BEAMS OF THE «A» AND «B» SERIES

Specimen	Concrete class	M_{crc}, kNm	Rebound deflection, mm	M_{ult}, kNm	f_{ult}, mm	$a_{crc,max}$, mm	$\varepsilon_{f,ult}$, με	Debonding type	Specimen failure behavior
Bla-1	B25	3.81	0.183	6.13	9.50	2.7	-	-	RR*
Bla-2	B25	3.91	-	7.45	19.84	2.0	-	-	RR+CCC
Bla-3	B25	4.27		6.92	21.43	2.0	-	-	RR*+CCC
Mean value		4.00	0.183	6.83	-	2.2	-	-	-
B1b-1	B25	4.28	-	10.05	14.29	1.1	12170	mixture	FRPR*
Blb-2	B25	5.07	-	10.42	11.16	0.5	11170	mixture	FRPR*
Blb-3	B20	4.33	0.206	10.25	8.30	1.0	13370	cohes.	FRPR
Blb-4	B30	5.40	0.257	10.10	8.08	0.9	12180	cohes.	FRPR
Blb-5	B20	4.32	0.218	11.07	9.78	1.1	15040	cohes.	FRPR
Mean (adhesive)	-	4.68	-	10.24	12.72	0.9	11670		-
Mean (cohesive)	-		0.227	10.47	8.72		13530		-
B2a-1	B35	4.74	-	6.98	10.60	1.5	-		RR*
B2a-2	B35	5.15	-	6.98	15.75	7.0	-		RR+CCC
B2a-3	B40	4.98	0.221	7.39	19.73	3.0	-		RR*+CCC
Mean value		4.96	0.221	7.12	-	2.2	-		-
B2b-1	B35	6.14	-	10.03	10.37	0.8	12180	mixture.	FRPR*
B2b-2	B40	5.79	-	10.19	12.52	1.6	10860	adhes.	FRPR*
B2b-3	B40	5.49	0.260	10.56	8.92	1.1	13790	cohes.	FRPR
B2b-4	B40	5.09	0.213	11.46	9.31	1.0	14280	cohes.	FRPR
B2b-5	B40	5.43	0.252	10.27	8.06	1.3	12190	cohes.	FRPR
Mean (adhesive)	-	5.59	-	10.11	11.44	1.1	11520	-	-
Mean (cohesive)	-		0.242	10.76	8.76		13420	-	-

Notes: RR reinforcement rupture, CCC - crushing of compressive concrete, RR* - reinforcement rupture sectional weakened spot welding, FRPR - midspan FRP rupture, FRPR* - FRP rupture sectional strap anchorage, mix. - mixed debonding, cohes.- cohesive debonding, adhes. - adhesive debonding

TABLE II
THE RESULTS OF STATIC TESTS OF BEAMS OF THE "C" SERIES

Specimen	Concrete class	Loading before the appearance of the first cracks and their grouting			Bending moment during reinforcement, kNm	Loading after the appearance of the first cracks and their grouting					Debonding type	Specimen failure behavior
		M_{crc}, kNm	Rebound deflection, mm	Maximum bending moment, kNm	$a_{crc,max}$, mm	M_{crc}, kNm	M_{ult}, mm	f_{ult}, mm	$a_{crc,max}$, mm	$\varepsilon_{f,ult}$, με		
Blc-1	B20	3.32	0.142	5.15	1.0	4.30	6.79	10.39	10.80	1.4	11680	cohes.	FRPR
Blc-2	B20	3.60	0.164	5.23	1.5	4.81	7.19	8.75	9.19	1.5	10190	cohes.	FRPR
Blc-3	B30	3.86	0.186	5.20	1.0	4.59	6.59	10.19	11.07	1.3	12760	cohes.	FRPR
Mean value	-	3.60	-	5.19	1.2	4.57	6.86	10.29	-	1.4	11540	-	-
B2c-1	B40	4.30	0.179	5.49	1.0	4.56	6.88	1137	10.29	1.1	14180	cohes.	FRPR
B2c-2	B40	4.92	0.214	5.64	0.9	4.79	7.02	9.03	9.75	1	8655	cohes.	RR*+ FRPR
B2c-3	B40	5.19	0.202	5.52	1.0	4.58	7.69	10.62	10.72	1.3	12430	cohes.	FRPR
Mean value	-	4.80	-	5.55	1.0	4.64	7.19	11.00	-	1.1	13305	-	-

Notes: RR* - reinforcement rupture sectional weakened spot welding, FRPR - midspan FRP rupture

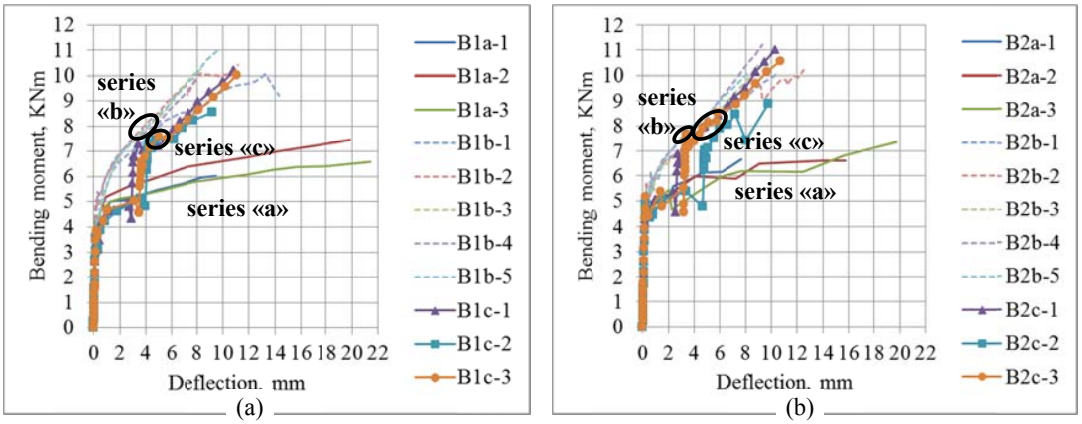

(a) (b)

Fig. 4 Bending moment–Deflection relationships for series «a», «b» and «c»: Group B1 (a), Group B2 (b)

TABLE III
THE RESULTS OF STATIC TESTS OF BEAMS OF THE "C" SERIES

Specimen	Binary card of defects	The relative area of the delamination, %		CFR strain, με
		Particular value	Average value	
B1b-3		7,8		10300
B1b-4		12,99	9,71	10660
B1b-5		8,34		10140
B1c-1		19,77		10280
B1c-2		22,59	22,93	8020
B1c-3		26,43		10240
B2b-3		11,78		10810
B2b-4		20,18	14,90	10200
B2b-5		12,73		10070
B2c-1		17,86		8970
B2c-2		33,08	32,41	7220
B2c-3		46,29		10450

The comparison of the experimental strain values, corresponding to the onset of cohesive delamination of CFRP, with the data theoretically obtained from 5 different methods used in practice, demonstrates a low reliability of these calculation methods (Fig. 5). For instance, the values calculated by the regulatory method used in Russia exceeds the experimentally registered by 15-75% for different classes of concrete.

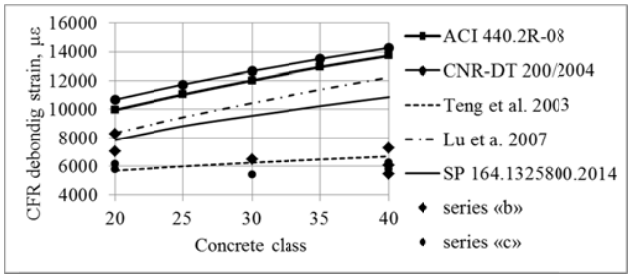

Fig. 5 The comparison of experimental and theoretical values of deformations corresponding to the onset of cohesive delamination

IV. CONCLUSION

1. It is shown that for the CFRP beams, which are destroyed due to the rupture of CFRP, their bearing capacity does not depend on the point when strengthening was performed. The bearing capacity of previously reinforced beams and beams reinforced during loading after the appearance of the first cracks and their grouting is higher by 37-39% and 38-49%, respectively, than the unreinforced beams. Grouting of cracks in beams under loading, allows to increase the limiting value of the bending moment by 45-71% compared to unreinforced beams.
2. It is established that for beams, reinforced during loading after grouting of the first cracks, the process of CFRP delamination begins at a strain by 4-65% lower, and the relative area of delamination is 2.1-2.3 times higher compared to beams, reinforced before loading.
3. The onset of delamination of CFRP sheet corresponds to the bending moment, which is 75% of the limit value. Thus, the presence of delaminations does not determine the limiting state of CFRP beams with anchorage of CFRP tape on the bearings. Therefore, it is possible to use the breaking strain of the composite as a limiting value of the deformations in the limit state design. The fact of cohesive delamination does not reduce the rigidity of the reinforced structure.

ACKNOWLEDGMENT

This research was supported by the Russian Science Foundation, project No. 14-29- 00172.

REFERENCES

[1] J.G. Teng. Failure modes of FRP-strengthened Restructures / 26th Conference on Our World in Concrete & Structures: 27 - 28 August 2001, Singapore. pp. 627-634..
[2] SP 164.1325800.2014. Strengthening of reinforced concrete structures with composite materials. Design rules.
[3] ACI 440.2R-08. Guide for the Design and Construction of Externally Bonded FRP Systems for Strengthening Concrete Structures. ACI. 2008.
[4] ZHANG Ai-hui JIN Wei-liang, LI Gui-bing, Behavior of preloaded RC beams strengthened with CFRP laminates. - Journal of Zhejiang University SCIENCE A, 2006 7(3), 436-444.
[5] K. Parikh, C.D. Modhera. Application of GFRP on preloaded retrofitted beam for enhancement in flexural strength. – International journal of civil and structural engineering, Volume 2, № 4, 2012, pp. 1070-1080.
[6] Y.A. Al-Salloum. Flexural behavior of rc beams strengthened with frp composite sheets subjected to different load cases. King Saud University, Saudi Arabia. http://faculty.ksu.edu.sa/ysalloum/Documents/My%20Papers/Flexure%20UK%202006.pdf.
[7] M. R. Valluzzi, E. Grinzato, C. Pellegrino, C. Modena. IR thermography for interface analysis of FRP laminates externally bonded to RC beams. Materials and Structures (2009) 42, pp. 25–34..
[8] A. Shirazi V.M. Karbhar, Quantifying defects and progression of damage in FRP rehabilitation of concrete through IR thermography. Asia-Pacific Conference on FRP in Structures (APFIS 2007). 2007 International Institute for FRP in Construction..
[9] F. Taillade, M. Quiertant, K. Benzarti, J.Dumoulin, Ch. Aubagnac. Nondestructive evaluation of FRP strengthening systems bonded on RC structures using pulsed stimulated infrared thermography / IFSTTAR, F-75015 Paris. pp. 193-208.
[10] Determination of thermography modes for recording delamination between composite material and reinforced concrete structures/ A.

Bykov, V. Matveenko, G. Serovaev, I. Shardakov, A. Shestakov // Problems of Deformation and Fracture in Materials and Structures: sel., peer rev. papers from the All-Russ. Conf. on Problems of Deformation and Fracture in Materials and Structures, June 17-19, 2015, Perm, Russia / Ed.: V. P. Matveenko, A. A. Tashkinov, D. A. Chinakhov. – Durnten-Zurich: TTP, 2016. – (Solid State Phenomena; vol. 243). - P. 97-104.